ISSN 1392 - 1207. MECHANIKA. 2010. Nr.1(81)

Investigation on thermo-acoustical instabilities related to a confined swirling burner

F. Bode*, R. Benea, V. Hodor*****

**Technical University of Cluj-Napoca, Department of Thermotechnics, Thermal Machines and Equipments, B-dul Muncii 103-105, 400641 Cluj-Napoca, Romania, E-mail: florin.bode@termo.utcluj.ro*

***Technical University of Cluj-Napoca, Department of Mechatronics, B-dul Muncii 103-105, 400641 Cluj-Napoca, Romania, E-mail: rbenea@gmail.com*

****Technical University of Cluj-Napoca, Department of Thermotechnics, Thermal Machines and Equipments, B-dul Muncii 103-105, 400641 Cluj-Napoca, Romania, E-mail: victor.hodor@termo.utcluj.ro*

1. Introduction

This study focuses on studying reacting and non-reacting flow in a nonpremixed swirl burner. In order to reduce harmful emissions, the current trend in burner designing is to operate under fuel lean and swirl combustion. Combustion efficiency and pollutant emissions of gas burners are strongly influenced by the fluid dynamics that controls mixture formation and chemical reactions [1].

Swirling lean nonpremixed flames are used in modern combustors because they offer the possibility of controlling flame temperature and thermal NO_x emissions. However, these flames pose a continuous challenge to engineers as they are unstable. They exhibit low frequency large-scale coherent structure and turbulent fluctuations [2-4]. These fluctuations could trigger non only noise, but undesirable combustion oscillations and structural damage.

By the use of swirl vanes which contribute to the creation of a tangential velocity component, a swirling flow will be generated. This swirling flow contributes to a better and fastest mixing of methane with air because of the induced turbulence and when the burning is taking place provides the flame stabilization.

This paper describes an investigation on the thermo-acoustic instabilities in swirling nonpremixed flame made by acoustic correlation between numerical simulation and experimental results. These instabilities arise as a direct consequence of the direct coupling between heat release fluctuations and combustor acoustics.

Many studies have been carried out to obtain deeper understanding and control of swirl combustion systems [5, 6], and numerical simulations of nonpremixed flames [7-11]. The phenomena are very complex as many physical, time and chemical scales are involved, therefore turbulent combustion instabilities constitutes a multi-scale 4D problem (space and time) [12]. The simulation of turbulent combustion is particularly difficult, as the phenomena involved are highly nonlinear and unsteady. The methane-air mixture flow and combustion will be analyzed using a RANS method. The closure assumptions of the *k-ε* model are only valid for high-intensity and nearly isotropic turbulence. In this case there are the zones where the turbulence is intense (mixing zone) and the zones where the flow is almost laminar [13-14]. Therefore for this simulation the turbulent flow model chosen was RNG *k-ε*.

The RNG-based *k-ε* turbulence model is derived from the instantaneous Navier-Stokes equations, using a mathematical technique called "renormalization group" (RNG) methods. It is similar in form to the standard k-ε model, but includes the following refinements: RNG model has an additional term in its ε equation that significantly improves the accuracy for rapidly strained flows, effect of swirl on turbulence is included in the RNG model, enhancing accuracy for swirling flows; the RNG theory provides an analytical formula for turbulent Prandtl numbers, while the standard *k-ε* model uses user-specified, constant values. While the standard *k-ε* model is a high Reynolds number model, the RNG theory provides an analytically derived differential formula for effective viscosity that accounts for low Reynolds number effects. These features make the RNG *k-ε* model more accurate and reliable for a wider class of flows than the standard *k-ε* model.

2. Experimental investigation

2.1. Experimental setup

A nonpremixed swirl burner of 50 kW capacity is used in the experimental investigations. The swirler consists of an outer part, with 8 swirl vanes which contribute to create a tangential velocity component for the primary air and a swirling flow will be generated.

In our work we have used an external sound board Creative Professional model E-MU0404USB (Premium 24-bit/192 kHz A/D and D/A converters* (A/D: 113 dB SNR, D/A: 117 dB SNR) E-MU XTC Class-A ultra-low noise Mic/Line/Hi-Z preamplifiers (-127 dB EIN) with 48 V phantom power and ground lift switches enable you to plug microphones ultra-low latency USB 2.0 drivers, hardware zero-latency direct monitoring (mono/stereo) allows to record and overdub with no annoying delay plug-and-play operation, cross-platform support (Windows XP/x64 and Mac OS X), and microphone AudioTechnica AT2010, 20 Hz-20 kHz, with line sensibility, unidirectional, capture solid angle 15°.

The audio signal was captured at a sampling rate of 44.1 kHz, which we found to be enough for this signal, audio sample size is 16 bit, and audio format is Pulse Code Modulation (PCM).

For each analyzed case, 30 audio signals with the length of 1.48 s randomly selected from the entire recorded audio signal (Fig. 1) were chosen. Fourier analysis for each of these samples was made.

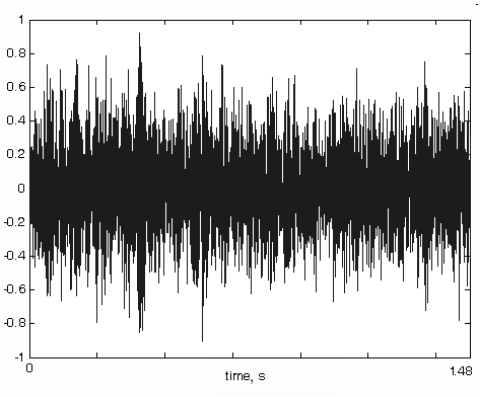

Fig. 1 Unprocessed sound signal

2.2. Nonreactive flow

To capture the ambient noise, the fan and the flow interaction with a solid structure, the audio signals captured in the nonreactive flow case were analyzed with Matlab using Fourier spectral analysis method. The results are presented in the next figure (Fig. 2). One can see that the most important spectral components are situated around 40 Hz and 300 Hz. The same frequencies can be seen in all 30 analyzed Fourier spectra.

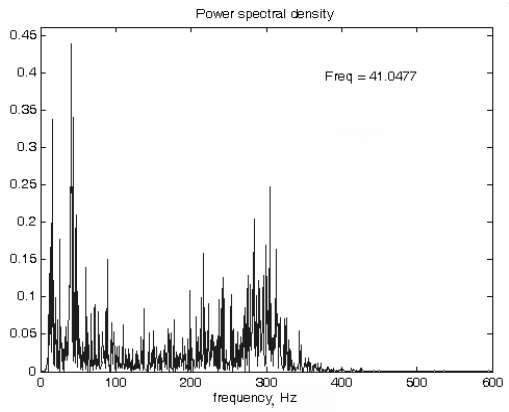

Fig. 2 Frequency distribution for the nonreactive flow

2.3. Reactive flow

The next figure (Fig. 3) presents one Fourier spectra for an audio signal captured in the methane-air reactive flow for lean combustion conditions. The dominant frequency in all the analyzed audio samples is around 300 Hz.

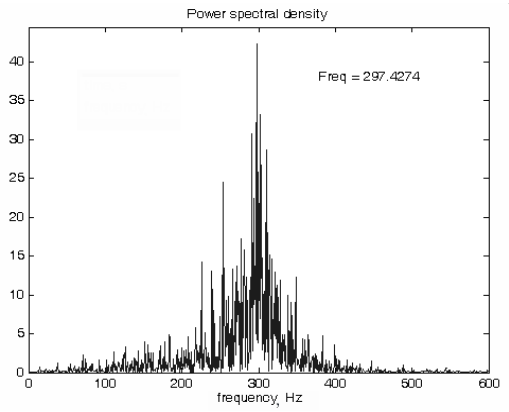

Fig. 3 Frequency distribution for the reactive flow for lean combustion conditions

The same analysis was performed in the reactive flow for near stoichiometric combustion conditions.

Fig. 4 presents one Fourier spectra for an audio signal captured in the methane-air reactive flow. The dominant frequency is around 300 Hz in all the analyzed audio samples.

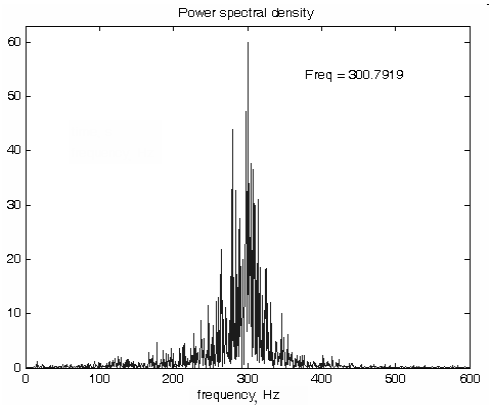

Fig. 4 Frequency distribution for the reactive flow for near stoichiometric combustion conditions

The same results were obtained after processing audio samples from the methane-air reactive flow for rich combustion conditions. There is only one important spectral component and is situated, the same, around 300 Hz (Fig. 5).

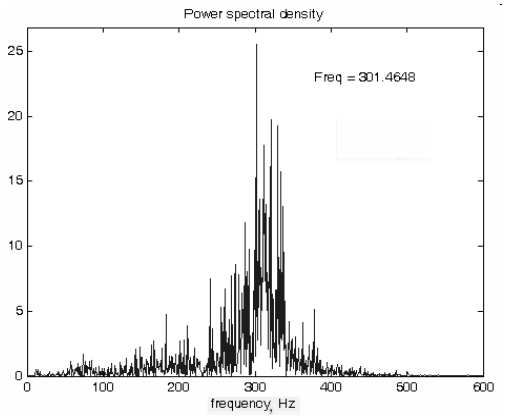

Fig. 5 Frequency distribution for the reactive flow for rich combustion conditions

The power spectral density is very low for the nonreactive flow case, compared with the reactive flow. Spectral sound analysis made with respect to the equivalence ratio reveals that frequency does not depend on the equivalence ratio.

In the Fig. 3 we can observe that under lean combustion conditions the frequency spread spectrum (more than 10% of maximum power) is the largest (240-340 Hz) and also has a tendency of being more intense for lower frequencies. The spread spectrum is narrower when the ratio is near stoichiometric (250-330 Hz) and also the frequency distribution is much closer to the Gaussian distribution (Fig. 4). In the rich combustion case (Fig. 5) we can observe that the frequency spectrum tends to get largest again (240-340 Hz), and its intensity has a tendency to move towards higher frequencies.

Under lean combustion conditions we found some other frequencies 225, 238, 258 and 280 Hz. For near

stoichiometric combustion conditions, some other dominant frequencies are 237, 247, 265 and 280 Hz and in the case of rich combustion case the dominant frequency is around 240, 260 and 285 Hz.

3. Numerical simulation

Having the real burner geometry from Fig. 6 we created the 3D geometrical model (Fig. 7) in Gambit [15]

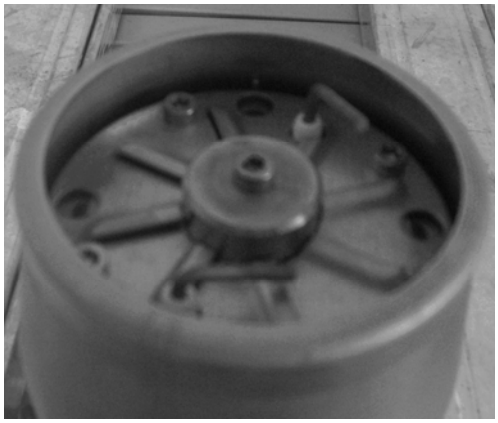

Fig. 6 Burner geometry

The grid consists of tetrahedral elements, a high density of elements being constructed in the interest zone (mixing zone, burner head) (Fig. 8). The total number of the elements is about 1.2 millions.

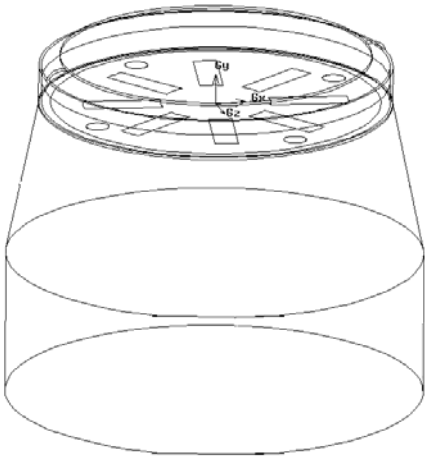

Fig. 7 Burner geometrical model

The studies were performed by the use of CFD software FLUENT [16]. A segregated solver formulation was used for these computations (equations are solved sequentially instead of simultaneously as in coupled solver). Using a control-volume based technique; Fluent converts the differential governing equations to linear algebraic equations that can be solved numerically. The control volume technique consists in integrating the governing equations for each control volume by obtaining discrete equations that conserve each quantity on a control volume basis. The solver stores the discrete values of the scalars at the cell centres and in order to determine the scalars value between the cells centres, second order upwind scheme for the momentum, swirl velocity, turbulent kinetic energy and turbulence dissipation rate were used for interpolation.

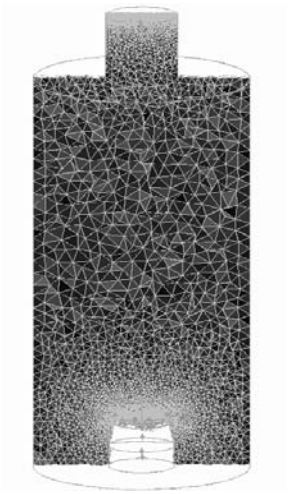

Fig. 8 Geometrical discretization

Regarding accuracy of results, we have imposed 10^{-4} convergence criteria for the residual energy balance, continuity, x-velocity, y-velocity, turbulent kinetic energy, dissipation rate and for the species. The governing equations represent the conservation of mass, momentum (Navier-Stokes), energy and additional species. Fluid properties are calculated from local gas composition. The RNG k-ε model with associated transport equations is applied to account for turbulence because of the different regions of the flow of low Reynolds number alternating with high turbulence zones. The combustion model used for this simulation is species transport with mixture material: methane-air-2step, the reaction is volumetric and the turbulence-chemistry interaction is eddy-dissipation. The standard wall functions option for the near wall treatment was applied as well as the no slip condition at the wall. The time step imposed was 0.001 s.

The pressure fluctuations in time in 7 points distributed as in Fig. 9 were monitored. First monitor point is located on the symmetry axis at 50 mm from the burner inlet. The second and third monitor points are placed on the same symmetry axis at 100 mm and 200 mm from the burner inlet. The following 4 monitored points are located in a plane situated at 50 mm from the inlets, monitor point four at 40 mm in OX direction and monitor point five at -40 mm in the same direction. Monitor point six is placed at 40 mm in the OZ direction and the last monitor point is positioned at -40 mm in the same direction.

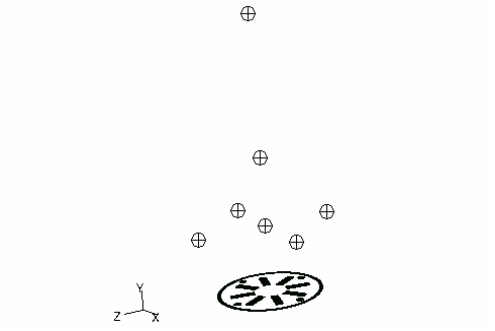

Fig. 9 Monitor points distribution

The evolution of the pressure in time for every monitor for 4.7 s in the nonreactive flow case and 3.5 s for the reactive flow case was recorded. In the nonreactive case, the flow has stabilized after 3.5 s, so the interval cho-

sen for Fourier analysis is from 3.5 to 4.7 s. The flow in the reactive case has stabilized after 1.5 s, so the chosen interval in this case for Fourier analysis is from 1.5 to 3.5 s.

In the next figures monitor 2 is being analyzed. For the nonreactive flow case, frequencies for the fluctuating pressure for monitor 2 are found around 6, 22 and 43 Hz (Fig. 10).

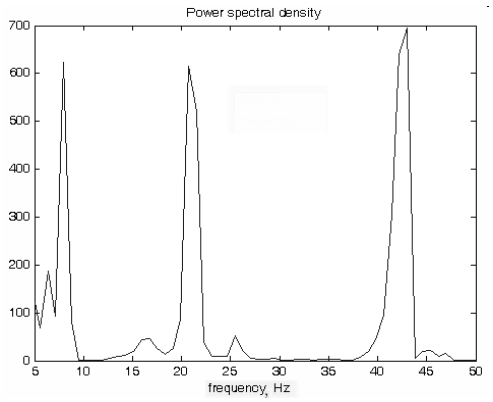

Fig. 10 Frequency distribution for the nonreactive flow for monitor point 2

For the reactive flow, fluctuating pressure frequencies are 6, 47, 236 Hz. The other frequencies are harmonics of the 47 Hz frequency (Fig. 11).

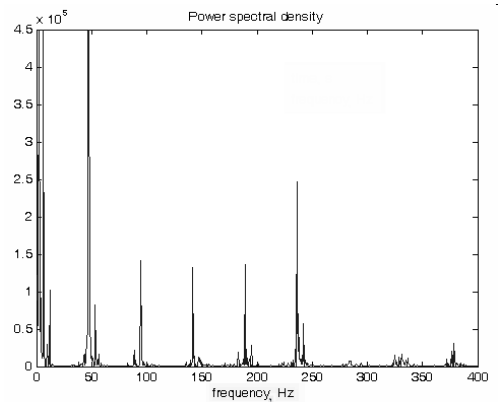

Fig. 11 Frequency distribution for the reactive flow for monitor point 2

In Fig. 12 pressure fluctuations for nonreactive flow over time for monitors 4-7 for a domain of 0.2 s are plotted.

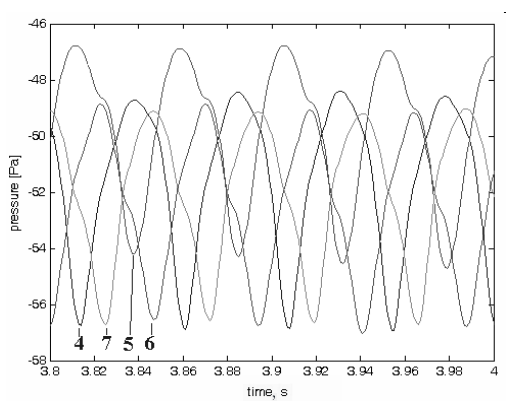

Fig. 12 Frequency distribution for the nonreactive flow for monitor point 2

In Fig. 13 pressure fluctuations for reactive flow over time for the same monitors for a domain of 0.1 s are plotted. It can be seen that intensity and frequency of pressure fluctuations are rising in the reactive flow case. In the case of nonreactive flow there is a clockwise succession of the monitors at 22 Hz frequency.

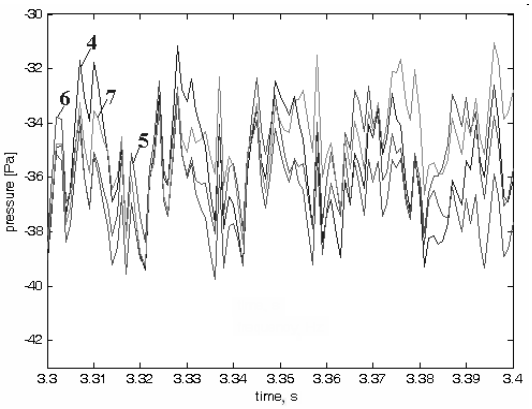

Fig. 13 Frequency distribution for the nonreactive flow for monitor point 2

From monitors 4-7 analysis, the conclusion was drawn that the pressure fluctuations frequencies for the nonreactive flow are around 22 Hz and 43 Hz (Fig. 14).

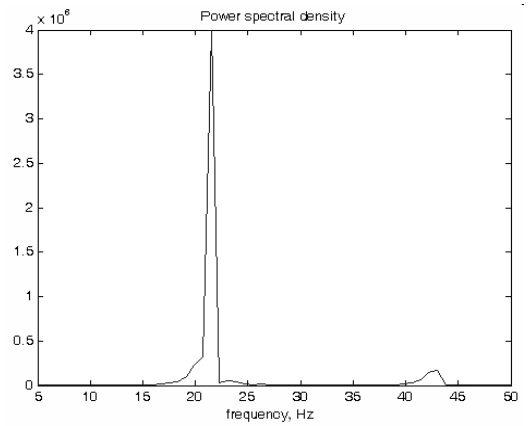

Fig. 14 Frequency distribution for the nonreactive flow for monitor 4

For the reactive flow, fluctuating pressure frequencies are 6, 47, 236 Hz. The other frequencies are harmonics of the 47 Hz frequency (Fig. 15).

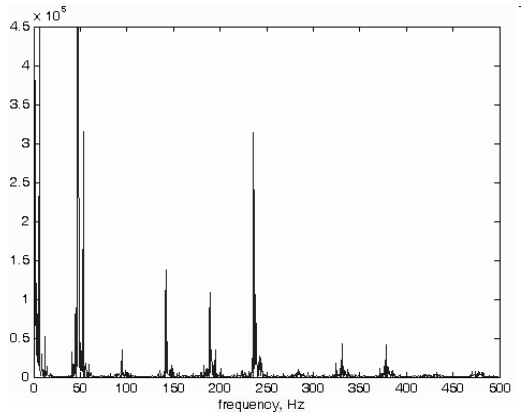

Fig. 15 Frequency distribution for the reactive flow for monitor 4

4. Conclusions

The power spectral density is insignificant for the nonreactive flow case, when compared with the reactive flow. Spectral sound analysis made with respect to the equivalence ratio reveals that frequency does not depend on the equivalence ratio.

Under lean combustion conditions the frequency spread spectrum (more than 10% of maximum power) is the largest (240-340 Hz) and also has a tendency of being more intense for lower frequencies. The spread spectrum is narrower when the ratio is near stoichiometric (250-330 Hz) and also the frequency distribution is much closer to the Gaussian distribution. In the rich combustion case we can observe that the frequency spectrum tends to get largest again (240-340 Hz), and its intensity has a tendency to move towards higher frequencies.

In the numerical simulation the pressure fluctuations over time in seven points distributed in the flow region near the burner head were monitored. A similarity in the nonreactive flow for experimental and numerical case for the frequency around 43 Hz was found. This frequency represents the nonreactive flow characteristics. For the experimental setup the 300 Hz frequency in the reactive and nonreactive case was recorded. In the nonreactive case the amplitude of the signal is much smaller. For the reactive flow in experimental setup it was found that the dominant frequency is around 300 Hz for all the studies made with respect to the equivalence ratio. This frequency seems to be the combustor internal frequency. The 300 Hz frequency appears in the nonreactive case and is amplified in the reactive flow case. Also it was found that other frequencies are around 240, 260, 280 Hz. In the numerical simulation in all studies a frequency around 6, 47 and 236 Hz for all the monitors was found.

5. Acknowledgement

This study is financed by the National Council for Higher Education Research (CNCSIS), the Executive Unit for the Funding of Higher Education and Academic Research (UEFISCSU), Romania, project IDEI, 1071/2007.

References

1. **Araneo, L., Coghe, A., Cozzi, F., Olivani, A., Solero, G.** Particle Image Velocimetry, book chapter: Natural gas burners for domestic and industrial appliances – Application of the Particle Image Velocimetry (PIV) Technique, ISBN 978-3-540-73527-4, 2008, p.245-257.
2. **Gupta, A.K., Lilley, D.G., Syred, N.**, Swirl Flows. -Abascus Press, 1984.-475p.
3. **Lucca-Negro, O., O'Doherty, T.** Vortex Breakdown: a review. -Progr. Energy and Combustion Science, 2001, v.27, p.431-481.
4. **Syred, N.** A review of oscillation mechanisms and the role of the precessing vortex core (PVC) in swirl combustion systems.-Progress in Energy and Combustion Science, 2006, v.32, p.93-161.
5. **Nogenmyr, K.-J., Fureby, C., Bai, X.S., Petersson, P., Collin, R., Linne, M.** Large eddy simulation and laser diagnostic studies on a low swirl stratified premixed flame.-Combustion and Flame, 2009, v.156, p.25-36.
6. **Demare, D., Baillot, F.** Acoustic enhancement of combustion in lifted nonpremixed jet flames.-Combustion and Flame, 2004, p.312-328
7. **Mahalingam, S., Thévenin, D., Candel, S., Veynante, D.** Analysis and numerical simulation of a nonpremixed flame in a corner.-Combustion and Flame, 1999, v.118, issues 1-2, p.221-232.
8. **Alekseenko, S.V., Dulin, V.M., Kozorezov, Y.S., Markovich, D.M.** Effect of axisymmetric forcing on the structure of a swirling turbulent jet.-International Journal of Heat and Fluid Flow, 2008, v.29, p.1699-1715.
9. **Peng, L., Zhang, J.** Simulation of turbulent combustion and NO formation in a swirl combustor.-Chemical Engineering Science, 2009, v.64, p.2903-2914.
10. **Kanga, D.M., Culicka, F.E.C., Ratner, A.** Combustion dynamics of a low-swirl combustor.-Combustion and Flame, 2007, v.151, p.412-425.
11. **Galpin, J., Naudin, A., Vervisch, L.** Large-eddy simulation of a fuel-lean premixed turbulent swirl-burner. -Combustion and Flame, 2008, v.155, p.247-266.
12. **Mikalauskas, R., Volkovas, V.** Investigation of adequacy of the acoustical field model. -Mechanika. -Kaunas: Technologija, 2009, Nr.2(76), p.46-49.
13. **Kačeniauskas, A.** Mass conservation issues of moving interface flows modelled by the interface capturing approach. -Mechanika. -Kaunas: Technologija, 2008, Nr.1(69), p.39-41.
14. **Benhamza, M.E., Belaid, F.** Computation of turbulent channel flow with variable spacing riblets. -Mechanika. -Kaunas: Technologija, 2009, Nr.5(79), p.36-41.
15. 2001, "GAMBIT 2 User's Guide", Fluent Inc.
16. 2001, "FLUENT 6 User's Guide", Fluent Inc.

F. Bode, R. Benea, V. Hodor

TERMOAKUSTINIŲ NESTABILUMŲ SŪKURINIAME PRISITAIKANČIAME DEGIKLYJE TYRIMAI

R e z i u m ė

Šiuolaikinėse degimo kamerose naudojama sūkurinė, iš anksto nemaišoma liesa liepsna. Ši liepsna jautri termoakustiniams degimo nestabilumams, kurie atsiranda dėl šilumos išsiskyrimo svyravimo ir degimo kameros akustikos. Termoakustiniai nestabilumai yra dinaminis reiškinys, pasireiškiantis daugumoje šiuolaikinių degimo sistemų dėl didelės amplitudės bei žemo dažnio slėgio ir šilumos išsiskyrimo svyravimo ir palaikomas automatiškai. Šiame straipsnyje atliekama degimo sūkurine, be iš anksto nemaišoma, liesa liepsna termoakustinių svyravimų nestabilumo išplėstinė analizė. Tyrinėjimai atliekami atsižvelgiant į termoakustinius degimo nestabilumus, priklausomus nuo stechiometrinio santykio, kartu taikant skaitinį šių nestabilumų įvertinimo metodą. Analizė atlikta taikant akustinę koreliaciją tarp skaitinio modeliavimo naudojant 3D RNG k-ε modelį, ir rezultatų, gautų eksperimentiniu būdu. Vyraujantys dažniai 20-50 Hz diapazone fiksuojami esant nereaktyviam tekėjimui ir 40-300 Hz diapazone – esant reaktyviam tekėjimui.

Siekiant įvertinti spektrinius duomenis, pašalinti nereikalingą aplinkos triukšmą, eksperimentiniams tyrimams panaudoti daugialypiai akustiniai jutikliai.

F. Bode, R. Benea, V. Hodor

INVESTIGATION ON THERMO-ACOUSTICAL INSTABILITIES RELATED TO A CONFINED SWIRLING BURNER

S u m m a r y

Swirling lean nonpremixed flames are used in modern combustors. These flames are susceptible of thermo-acoustic combustion instabilities, caused by the coupling between heat release fluctuations and combustor acoustics. Thermo-acoustic instabilities are dynamic phenomena that represent a major threat for most modern combustion systems. It consists of the coupling and autosustenance of large amplitude and low frequency pressure and heat release oscillations. Analysis of thermo-acoustic combustion instabilities of a nonpremixed swirling flame is presented extensively in this paper. This study is concerned with the evaluation of the influences induced by the equivalence ratio on the thermo-acoustic combustion instabilities, as well with a numerical method for determining these instabilities. This analysis is made by acoustic correlation between numerical simulation using the 3D RNG k-ε model and experimental results. The dominant frequencies are located in the ranges 20-50 Hz for the nonreactive flow, and 40-300 Hz for the reactive flow. Multiple acoustic sensors are used in the experimental setup in order to account for spectral acquisition and to help eliminate the irrelevant environmental noise.

Ф. Боде, Р. Венея, В. Годор

ИССЛЕДОВАНИЕ ТЕРМО-АКУСТИЧЕСКИХ НЕСТАБИЛЬНОСТЕЙ В ПРИСПОСОБЛЯЕМОЙ ВИХРЕВОЙ ГОРЕЛКЕ

Р е з ю м е

В современных камерах сгорания используется худое вихревое пламя без предварительного смешивания. Она чувствительна к термоакустическим нестабильностям сгорания, которые появляются вследствие колебаний теплоотдачи и акустических свойств камеры сгорания. Термоакустическая нестабильность – это динамическое явление, которое обнаруживается во многих современных системах сгорания. Оно появляется и автоматически поддерживается давлением большой амплитуды и низкой частоты, и колебаниями теплоотдачи. В статье проводится расширенный анализ термоакустических колебаний сгорания при вихревом худом пламени без предварительного смешивания. Исследования проведены учитывая нестабильности термоакустического сгорания, зависящие от стехиометрического соотношения вместе с числовым методом, предназначенным для оценки указанных нестабильностей. Анализ произведен с помощью акустической корреляции между результатами, полученными методом числового моделирования, используя модель 3D RNG k-ε и экспериментальных данных. При наличии нереактивного течения преобладающие частоты фиксировались в диапазоне 20-50 Hz. При реактивном течении преобладающие частоты занимают диапазон 40-300 Hz. Стараясь оценить спектральные данные, устранить ненужный шум окружающей среды, для экспериментальных исследований использованы разносторонние акустические датчики.

Received August 21, 2009
Accepted January 07, 2010

DOI: 10.5755/j02.mech.9757